Unified View of Sediment Transport by Currents and Waves. III: Graded Beds

Leo C. van Rijn[1]

Abstract: The problem of suspended load and bed load transport in river and coastal flows over graded beds is addressed. Two effects are important: the degree of exposure of the sediment particles of unequal size within a mixture (hiding of smaller particles resting or moving between the larger particles) and the nonlinear dependence of transport on particle diameter. The former effect can be modeled by modifying the critical bed-shear stress through a correction factor and by modifying the effective grain roughness through another correction factor. The modeling of the effective bed-shear stress parameter is studied by using various alternative methods. Based on comparison with suspended load and bed load transport data for graded beds in steady and oscillatory flow, the most promising method is selected. The proposed prediction method is found to work well for the fine sand bed range as well as the coarse sand-gravel bed range.

DOI: 10.1061/(ASCE)0733-9429(2007)133:7(761)

CE Database subject headings: Sediment; Currents; Bed loads; Rivers; Coastal environment.

Introduction

The sediment beds of rivers, estuaries, and coastal seas usually exhibit a large horizontal variation of sediment sizes. Local variations related to the presence of bed forms (differences in size at the top and in the trough) may occur, but horizontal sorting due to selective transport processes is a more important process in nature (fining in downstream direction). Vertical sorting is the process governing the vertical exchange of sediment particles between the various bed layers and between the bed surface material and the suspension. Experimental results of graded bed materials show that the transport of the finer fractions often is slightly dominant [see Fig. 11 of this paper for steady flow and Fig. 4.6 of Sistermans (2002) for oscillatory flow]. Sistermans (2002) also shows that the suspended sediment diameters of graded bed material are significantly smaller than those in the case of almost uniform bed material. Strong vertical sorting effects do occur between the graded bed material and the suspension; the depth-mean value of the suspended sediment size was much smaller (factor of 2 to 3) than the mean bed material size (Sistermans 2002). These sorting effects can only be represented by taking into account the full size composition multifraction approach (MF) method) of the graded bed material, which may vary horizontally and vertically.

A first understanding of the difference in transport rate according to the multifraction (MF) method and the single-fraction approach (SF) method can be obtained by using a simple transport formula of the type $q_s \approx \Sigma p_i d_i^{\alpha} u^3$ (u=velocity; d_i=diameter; and p_i=percentage of fraction i of bed material sample). The exponent α may vary between $\alpha=-2$ or $\alpha=2$. The effect of hiding is neglected. In both companion papers (Van Rijn 2007a,b), it has been shown that measured bed load transport rates are almost independent of particle size and that suspended transport rates are proportional to d^{-2}.

Taking $\alpha=-2$ and a symmetric size distribution ($N=7$ fractions), as follows:

$$p_1 = 0.05, \quad p_2 = 0.15, \quad p_3 = 0.2, \quad p_4 = 0.2, \quad p_5 = 0.2,$$

$$p_6 = 0.15, \quad p_7 = 0.05$$

$$d_1 = 0.5d, \quad d_2 = 0.666d, \quad d_3 = 0.8d, \quad d_4 = 1d,$$

$$d_5 = 1.25d, \quad d_6 = 1.5d, \quad d_7 = 2d$$

the MF transport can be expressed in terms of the SF transport yielding: $q_{s,N=7}=1.26q_{s,N=1}$ for all current velocities. Taking a wider (symmetric) size distribution with $d_1=0.25d$; $0.5d$; $0.75d$; $1d$; $1.33d$; $1.5d$; $2d$; and $d_7=4d$ with similar percentages, it follows that $q_{s,N=7}=2.1q_{s,N=1}$.

Thus, if the transport rate is proportional to d^{-2}, the application of the MF method (without the hiding effect) yields a larger transport rate than that based on the SF method with a representative diameter d. Further, the wider the size distribution, the larger is the effect.

When the transport rate is proportional to d^2 ($\alpha=2$) instead of d^{-2}, the MF method also yields $q_{s,N=7}=1.26q_{s,N=1}$ (or $q_{s,N=7}=2.1$ $q_{s,N=1}$ for a wider size distribution). Thus, the transport rates are the same, but in the latter case (q_s proportional to d^{-2}) the transport of finer particles is dominant (suspended load) in the transport process, whereas in the former case (q_s proportional to d^2) the transport of coarser particles is dominant.

In natural conditions the bed material generally has a slightly asymmetric size distribution. Further, hiding and sorting processes do occur, which should be taken into account. The effect of these phenomena on the transport process of graded sediment is not quite clear. The transport rate of graded sediment may increase or decrease compared to the transport rate of "uniform" sediment of the same median diameter (d_{50}). The modeling of transport

[1]Senior Engineer, Delft Hydraulics, P.O. Box 177, Delft 2600 MH, The Netherlands; and, Professor, Univ. of Utrecht, P.O. Box 80115, Utrecht 3508TC, The Netherlands.

Note. Discussion open until December 1, 2007. Separate discussions must be submitted for individual papers. To extend the closing date by one month, a written request must be filed with the ASCE Managing Editor. The manuscript for this paper was submitted for review and possible publication on July 8, 2005; approved on August 2, 2006. This paper is part of the ***Journal of Hydraulic Engineering***, Vol. 133, No. 7, July 1, 2007. ©ASCE, ISSN 0733-9429/2007/7-761–775/$25.00.

processes for graded sediments using a MF method based on the TR2004 Model is explored in this paper, focusing on the fine sand range (62–500 μm). The coarse sand and gravel range was studied by Kleinhans and Van Rijn (2002) based on a stochastic prediction method to account for the fact that the transport regime of gravel-bed rivers is slightly below or just above incipient motion.

Hiding and Exposure Processes: Critical Bed-Shear Stress

Grain sorting is related to the selective movement of sediment particles in a mixture near incipient motion at low bed-shear stresses and during generalized transport at higher shear stresses. Two effects are important:

1. The degree of exposure of sediment particles of unequal size within a mixture (hiding of smaller particles resting or moving between the larger particles); this effect can be modeled:
   - By modifying the critical bed-shear stress through a correction factor $\xi_i = F(d_i/d_{50})$, as proposed by Egiazaroff (1965); and
   - By modifying the effective grain shear stress through a correction factor $\lambda_i = F(d_i/d_{50})$ acting on the bed particles, as discussed by Day (1980); the grain roughness of a mixture is not quite clear; the grain roughness may be related to the individual fraction size d_i or to the larger particles d_{90} of the mixture.
2. The nonlinear dependence of transport on particle diameter, for example: Suspended load transport is inversely proportional to grain size; $q_s \approx d^m$ with m coefficient between −0.5 and −2 (see Van Rijn 2007b); bed load transport may increase weakly with grain size in the fine particle range (between 100 and 500 μm) and may decrease with grain size for coarse particles (larger than 500 μm, see Van Rijn 2007a).

The degree of exposure of a grain with respect to surrounding grains obviously is the most important parameter determining the bed-shear stress for initiation of motion, as shown by Fenton and Abbott (1977). They studied the effect of relative protrusion (p/d) on the initial movement of grains in the transitional and fully turbulent regime; p=protrusion of a particle above others; and d=diameter. Test grains were placed on top of a rod between similar grains glued to the flume bottom. The rod was then screwed upwards, pushing the grain into the flow until it was swept away. This was repeated 20 times for each test. Two types of grains were used: 2.5 mm diameter angular polystyrene grains and 5 to 10 mm well-rounded pea gravel. Relative protrusion was varied in the range between −0.2 and 0.8. A negative relative protrusion is a configuration with the top of the grain below that of the adjacent grains. The maximum relative protrusion of 0.8 is that of a grain sitting above one of the interstices formed by the other grains. The critical bed-shear stress for incipient motion (compared to that for zero protrusion $p=0$) was found to decrease for increasing positive relative protrusion and to increase for negative relative protrusion values. From a comparison of the data of Fenton and Abbott and the data of Shields, it follows that the Shields curve represents conditions with relative protrusions in the range of 0.1 for larger particles to 0.3 for smaller particles.

Carling (1983) found that relative protrusion is an important parameter for large grain sizes in natural shallow streams with poorly sorted bed material (between 0.2 and 200 mm). The threshold values decreased for increasing relative protrusion (expressed as d_5/h; d_5=mean size of 5 largest grains of sample; h=flow depth) in the range of 0.1–0.5. For steady flow in gravel-bed rivers some researchers (Parker et al., 1982) have found that all sizes in a mixture begin moving at nearly the same bed-shear stress (equal mobility concept).

Wilcock and McArdell (1993) performed laboratory experiments with bimodal sand-gravel mixtures ($d_{10} \cong 0.3$ mm; $d_{50} \cong 8$ mm; and $d_{90} \cong 30$ mm) and derived the critical bed-shear stress for incipient motion from fractional transport rates. Their findings are:

1. At the lowest flows (0.4 m/s at depth of about 0.1 m) the transport is composed almost entirely of sand sizes (<2 mm), organized into irregular flow-parallel stripes;
2. As flow increases over this low-transport range, the bed coarsens because the surface pores are progressively filled with sand;
3. As flow strength increases to the upper regime, an increasing proportion of the gravel fractions are entrained into transport and long, narrow dune-type bed forms develop; the body of the bed forms (length=1 m, height=0.02 m) consists of sand grains (<1 mm); most grains are deposited in the region of the advancing front; gravel grains move as single grains and rapidly traverse the bed form without stopping; the largest gravel grains often overpass several bed forms; the finest sand fractions move over the bed form in suspension; and
4. At relatively high flow strengths (1 m/s at depth of 0.1 m) the bed surface becomes consistently finer, because more fine sand is made available for transport (not sheltered anymore by the gravel grains).

The fractional transport rates (scaled by their proportion on the bed surface) were observed to fall into two groups: one consisting of fully mobilized finer grains moving at a more or less constant fractional transport rate and another consisting of immobile or partially mobile coarser grains moving at much smaller transport rates. The grain size separating (partially) mobile and immobile grains increases with increasing flow strength from about 0.5 to 10 mm. Complete mobilization of a certain size fraction occurs at roughly twice the bed-shear stress necessary for incipient motion. Fully mobile is defined as $p_i/F_i > 1$, with p_i=proportion of each fraction in the transported material and F_i=proportion of each fraction on the bed surface. The bed-shear stress for incipient motion of the sand particles (0.3–1 mm) was approximately constant at about 0.5 N/m^2; the values of the gravel grains (1–70 mm) were found to increase from 0.5–7 N/m^2.

Wilcock (1993) and others analyzed measured transport rates of individual fractions for conditions just beyond initiation of motion. The fractional bed load transport rates ($q_{b,i}$) are normalized to their availability (F_i) in the bed material and plotted as a function of the bed-shear stress ($q_{b,i}/F_i$ against τ_b). A small threshold transport (say 0.0001 kg/s/m) is introduced as an objective threshold criterion to find the threshold bed-shear stress for initiation of motion ($\tau_{b,\mathrm{cr},i}$) of each particular fraction. Wilcock studied the critical bed-shear stress of individual size fractions in unimodal and bimodal sediments. Flume and field data from the literature and new flume data were analyzed. The fluid bed-shear stress was defined as the skin-friction stress when bed forms were present.

Petit (1994) studied the motion of marked individual gravel particles (d_{50} between 12 and 39 mm) in a flume. The bed-shear stresses were evaluated from measured near-bed velocity gradients, when initial movement of marked particles was observed to occur. Two types of movements were defined: initiation of movement (about 20% of the bed surface in motion) and generalized

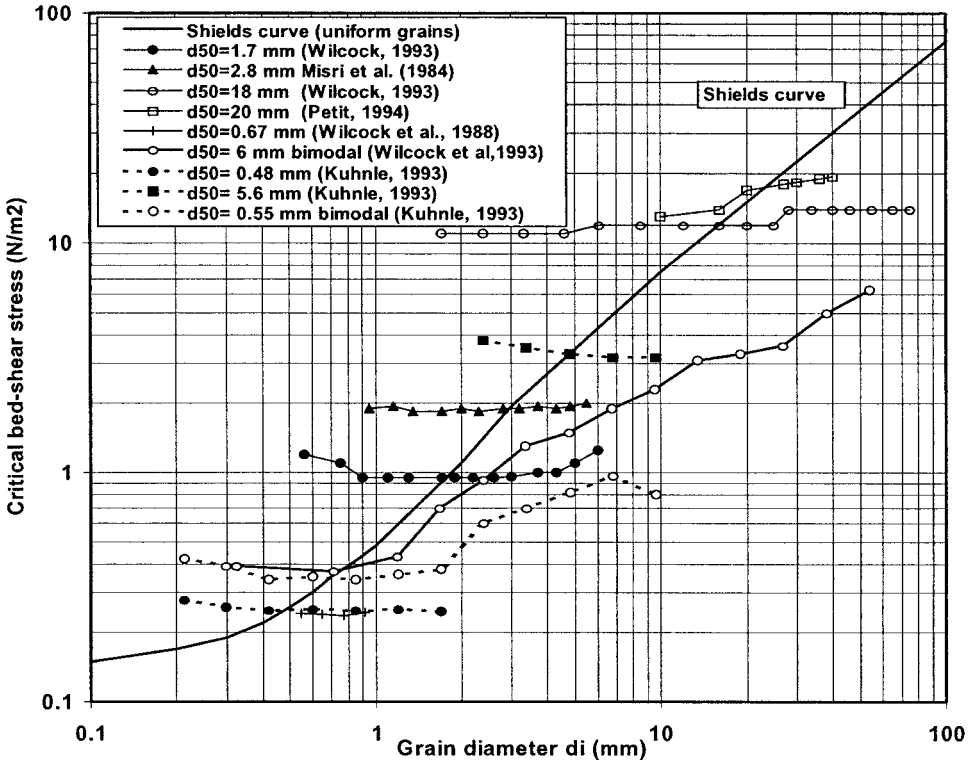

Fig. 1. Critical bed-shear stress of individual size fractions in a mixture as a function of grain diameter [adapted from Wilcock (1993)]

movement. Flume runs were conducted with different slopes and discharges. Before each run, the marked particles of different sizes were arranged on the bed at different locations along the flume. The particles were placed on a bed consisting of similar particles. Velocity measurements were done at these locations at moments of movement. The bed-shear stresses derived from the measured velocity gradients were plotted as a function of particle diameter. The data showed the presence of two or more parallel curves representing an upper and a lower limit. The upper limit represents the limit of shear stress above which movement of material is certain (all marked particles in motion); the lower limit represents the limit of shear stress below which movement is rare (80% of particles in rest).

Fig. 1 shows the critical bed-shear stress as a function of particle diameter based on the results of Misri et al. (1984), Wilcock (1993), Wilcock and Southard (1988), Petit (1994), and Kuhnle (1993) for unimodal sediment (sand or gravel) mixtures and Wilcock and McArdell (1993) and Kuhnle (1993) for bimodel (sand and gravel) mixtures. The Shields curve for uniform sediment is also shown. The data of Petit represent the average value of the two limiting shear stresses.

Most of the data in Fig. 1 refer to relatively coarse sediment material ($d > 1$ mm). The data sets show a slight increase of the critical bed-shear stress for the coarser fraction sizes within the unimodal mixture and a relatively strong increase of the critical bed-shear stress for the bimodal mixtures. The finest fractions ($d_i < 1$ mm) of the Wilcock (1993) mixtures and the Kuhnle (1993) mixtures also seem to have a somewhat higher critical shear stress. The data sets of Wilcock and Southard (1988) and Kuhnle (1993) for unimodal mixtures show an almost constant critical bed-shear stresses (horizontal line) for sand in the range of 0.5–2 mm. A horizontal line in Fig. 1 implies equal mobility of all size fractions; all grain sizes of the mixture are set into motion at the same bed-shear stress. In that case the composition of the transported bed load particles is the same as that of the original bed material under all conditions. Based on the data of Fig. 1, the concept of equal mobility may be reasonably correct for unimodal (sand or gravel) sediments between 0.2 and 10 mm. The curves cross the Shields curve (uniform sediment) at approximately the median diameter (d_{50}), except for the data set of Wilcock and Southard (1988). As regards the data crossing the Shields curve, the larger sizes are set into motion at bed-shear stresses that are smaller than required for uniform material of the same size, whereas the smaller size fractions require higher bed-shear stresses than for uniform material of the same size. The reason for this is that the larger sizes within a mixture are more exposed to the flow, whereas the smaller sizes tend to be sheltered from the flow by the larger particles. Thus, the larger particles of a mixture are substantially more mobile than the same particles of uniform bed material.

Kuhnle (1993) performed experiments with bimodal sand-gravel mixtures; the percentages of gravel were varied (10, 25, and 40%). The mobility of the sand particles was not found to change much for increasing percentages of gravel, but the mobility of the gravel particles decreased rapidly for increasing percentage of gravel. Thus, bimodal sediment shows combined behavior of uniform and mixed sediment. If the bed sediment is more bimodal, then the sand and gravel fractions show different behavior. The gravel fractions show slightly size-selective transport, while the sand part shows equal mobility.

These trends found for bimodal sediment cannot be explained with a simple hiding-exposure concept assuming that the bed surface is thoroughly mixed. A more plausible explanation is local size segregation in the form of longitudinal sand ribbons on gravel beds, which have been observed in all considered experiments. If fine sediment is concentrated in more or less homogeneous patches, then the critical shear stress will approach that of uniform sediment. The hiding-exposure phenomenon then acts to

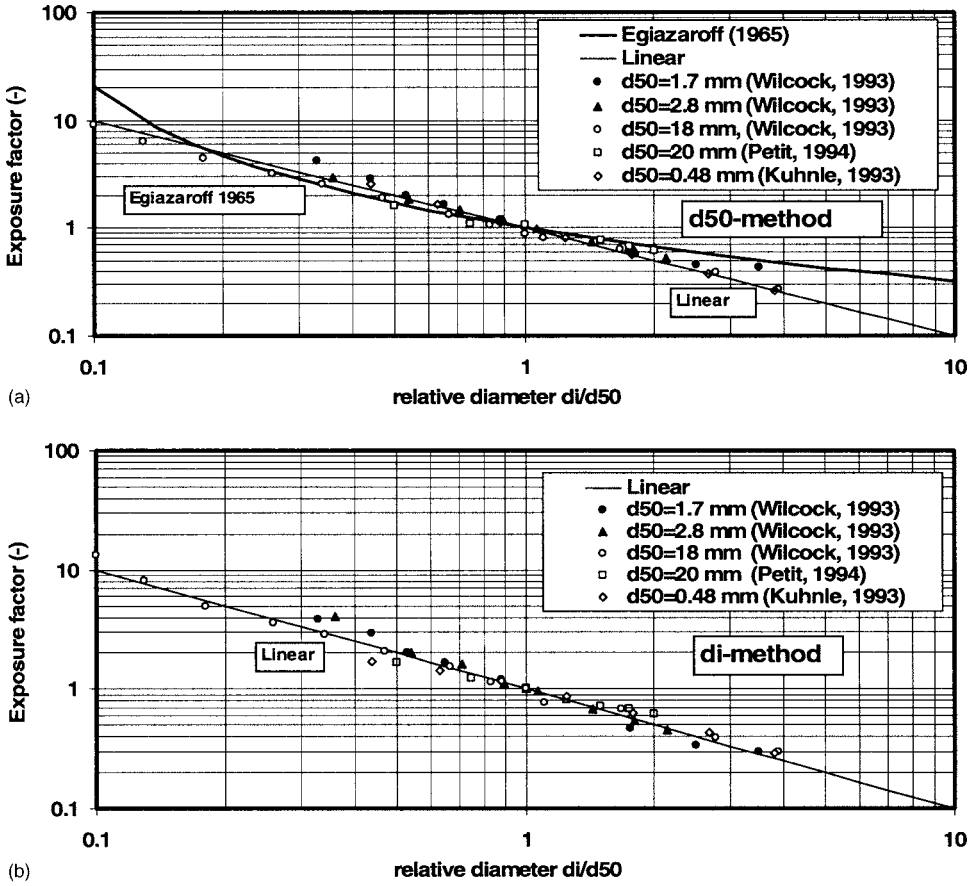

Fig. 2. Hiding exposure factors: (a) hiding-exposure factor based on d_{50} method; (b) hiding-exposure factor based on d_i method

such extent that the sediment within a sand patch exhibits equal mobility. The coarse fractions of the bed surface will be more exposed than in the case of uniform coarse material, resulting in relatively large critical bed-shear stress but still considerably smaller than for the uniform coarse material (considerably below the Shields curve). Part of the coarse material is buried beneath the fine patches, which decreases the transport rate of the coarse material.

Komar (1996) states that the selective mobility pattern of fine sand material is opposite to that found in coarser gravel material. In sandy bed material the entrainment of the finest fractions is caused by relatively large bed-shear stresses (curve sloping upward to the left, see Fig. 1). Thus, in the sand-size range the larger grains may be selectively removed, leaving behind the finer grains. The data set of Rakoczi (1975) concerning sandy materials (0.5 mm) show that the finer grains are eroded before the medium and coarser grains are set into motion (Rakoczi 1975). This latter behavior is opposite to the findings of Komar. More experimental data in the fine sand range is needed to better determine the critical bed-shear stress of mixtures in the fine sand range.

The available data of Fig. 1 can be used to derive the exposure or hiding factor (ξ) for particles in a mixture. Two approaches are possible:

1. d_{50} method introduced by Egiazaroff (1965); the hiding factor is defined as the ratio of the dimensionless critical bed-shear stress of fraction diameter d_i and the dimensionless critical bed-shear stress according to Shields based on the median diameter d_{50} [see Eq. (1*a*)]; it is noted that Egiazaroff actually used the mean diameter (d_m)

$$\xi_{i,\theta} = \theta_{\mathrm{cr},i}/\theta_{\mathrm{cr},d_{50},\mathrm{Shields}} = (\tau_{b,\mathrm{cr},i}/\tau_{b,\mathrm{cr},d_{50},\mathrm{Shields}})(d_{50}/d_i) = F(d_i/d_{50}) \quad (1a)$$

The critical bed-shear stress becomes

$$\tau_{b,\mathrm{cr},i} = \xi_{i,\theta}(d_i/d_{50})\tau_{b,\mathrm{cr},d_{50},\mathrm{Shields}} \quad (1b)$$

2. d_i method; the hiding factor is defined as the ratio of the dimensionless critical bed-shear stress of fraction diameter d_i and the dimensionless critical bed-shear stress according to Shields based on the fraction diameter d_i

$$\xi_{i,\tau} = \theta_{\mathrm{cr},i}/\theta_{\mathrm{cr},d_i,\mathrm{Shields}} = \tau_{b,\mathrm{cr},i}/\tau_{b,\mathrm{cr},d_i,\mathrm{Shields}} = F(d_i/d_{50}) \quad (2a)$$

The critical bed-shear stress becomes

$$\tau_{b,\mathrm{cr},i} = \xi_{i,\tau}\tau_{b,\mathrm{cr},d_i,\mathrm{Shields}} \quad (2b)$$

in which $\tau_{b,\mathrm{cr},i}$=critical bed-shear stress of fraction d_i within a mixture; $\tau_{b,\mathrm{cr},i,\mathrm{Shields}}$=critical bed-shear stress of fraction d_i based on Shields curve; $\tau_{b,\mathrm{cr},d_{50},\mathrm{Shields}}$=critical bed-shear stress of d_{50} based on Shields curve; and θ=dimensionless critical bed-shear stress=$\tau_{b,\mathrm{cr}}/[(\rho_s-\rho)gd]$.

The data of Fig. 1 have been used to compute the hiding-exposure factor values, which are shown in Fig. 2. The hiding factor or exposure factor of Egiazaroff (1965), defined as a multiplication factor to the dimensionless critical shear stress, is given by

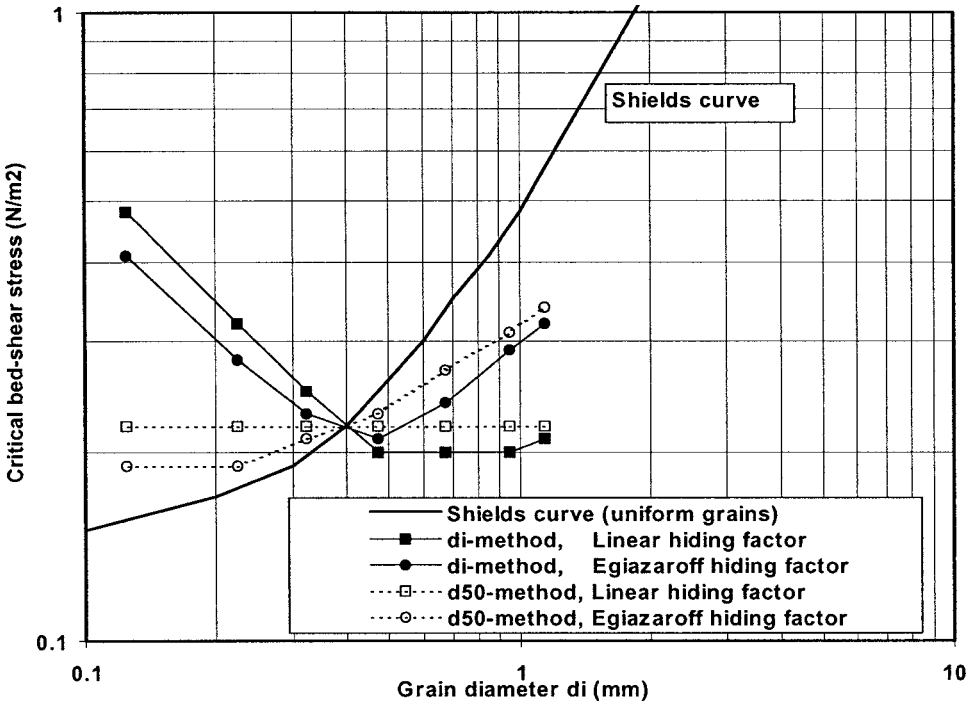

Fig. 3. Computed critical bed-shear stress for fractions of 400 μm mixture using four different methods

$$\xi_{i,\theta} = \theta_{\mathrm{cr},i}/\theta_{\mathrm{cr},d_{50}} = [\log(19)/\log(19d_i/d_{50})]^2 \quad (3)$$

and is also shown in Fig. 2(a). Originally, Egiazaroff used the average diameter d_m in Eq. (2) instead of d_{50}. In the present approach the d_{50} is used to be consistent with the single fraction transport formulas in which generally the d_{50} value is being used as the representative parameter.

The hiding factor of Egiazaroff yields values which are somewhat too large for the finest fractions ($d_i/d_{50}<0.2$) and also for the coarsest fractions ($d_i/d_{50}>3$). The data in Fig. 2(a) can be represented reasonably well by a linear expression: $\xi_{i,\theta}=(d_i/d_{50})^{-1}$. The hiding factor data based on the d_i method (Fig. 2(b) can be very well represented by a linear expression: $\xi_{i,\tau}=(d_i/d_{50})^{-1}$.

Buffington and Montgomery (1997) have presented an extensive overview of the most frequent empirical hiding factors. They conclude that no universal relation can be found.

In this paper attention is focused on the fine sand range and, therefore, the hiding-exposure factors of Fig. 2 have been applied to a graded bed with a d_{50}=400 μm; d_{15}=75 μm; and d_{95}=1,150 μm. The results are shown in Fig. 3. The application of the d_i method for mixtures in the fine sand range results in an increase of $\tau_{b,\mathrm{cr},i}$ for decreasing fraction diameter (<400 μm) as a consequence of the form of the Shields curve for smaller diameters and the relatively large hiding factors for small d_i/d_{50} values. As can be seen, the $\tau_{b,\mathrm{cr},i}$ parameter is about constant for the fractions with diameters larger than about 400 μm when the linear hiding factor is used. Comparison with measured data is required to select the most realistic method. In the absence of fine sediment data, Eq. (3) of Egiazaroff is herein supposed to give the most realistic results for fine sediments, because it has a theoretical basis and will therefore be used as the standard approach in the MF method.

Suspended Load Transport: Multifraction Approach

Definition of Bed-Shear Stress Parameter

Generally, the approach is to divide the bed material in a number of size fractions and to compute the sand transport rate of each size fraction using an existing single fraction transport model (replacing the median diameter of the bed material by the mean diameter of each fraction) with a correction factor (ξ_i and/or λ_i) to account for the nonuniformity effects. These corrrection factors are necessary because the coarser particles are more exposed to the near-bed steady and oscillatory flow (current and wave motion) than the finer particles which are somewhat sheltered by the coarser particles (hiding effect). The interaction of the size fractions can be represented by increasing the critical shear stress of the finer particles and decreasing the critical shear stress of the coarser particles. Thus, coarse particles are more easily entrained in the case of a graded bed than in the case of a bed consisting of uniform, coarse sediment. Herein, the theoretical correction factor of Egiazaroff (1965) is used to correct the critical bed-shear stress. Armoring may occur if the coarser particles are immobile, whereas the smaller grains are eroded (despite their increased critical bed-shear stress) until the developing armor layer prevents further pick-up of finer underlying sediments. During higher flow velocities the armor layer may also be mobilized (mobile armor layer). Bed forms of finer sediments may migrate over the coarser armor layer. Armoring is herein neglected, given the near-equal mobility and relatively narrow grain-size distribution of common sand mixtures.

In addition, the correction factor (λ_i) of Day (1980) is considered. Based on his findings, the effective grain-shear stress should also be modified because the fraction particles experience a different effective fluid drag as the smaller particles are hiding between the larger ones and the larger particles are more exposed.

Table 1. Bed Material Composition for 40, 200, 400, and 800 μm Bed Mixtures (d_{10}, d_{90} between Parentheses)

40 μm (12, 95)			200 μm (90, 310)			400 μm (160, 860)			800 μm (200, 1835)		
Fraction (μm)	d_i (μm)	p_i (%)	Fraction (μm)	d_i (μm)	p_i (%)	Fraction (μm)	d_i (μm)	p_i (%)	Fraction (μm)	d_i (μm)	p_i (%)
8–16	12	10	50–100	75	5	75–175	125	5	100–200	150	5
16–31	24	20	100–150	125	15	175–275	225	15	200–500	300	15
31–48	39	20	150–200	175	20	275–375	325	20	500–700	600	20
48–62	55	20	200–250	225	20	375–575	475	20	700–1,300	1,000	20
62–125	94	20	250–300	275	20	575–775	675	20	1,300–1,700	1,500	20
125–250	187	10	300–350	325	15	775–1,125	950	15	1,700–2,300	2,000	15
			350–450	400	5	1,125–1,175	1,150	5	2,300–2,700	2,500	5

The total sand transport rate and the total sediment concentration (c) for all size fractions can be obtained by summation of the transport rates per fraction taking the probability of occurrence of each size fraction into account, as follows:

$$q_b = \Sigma p_i q_{b,i}, \quad q_s = \Sigma p_i q_{s,i}, \quad c = \Sigma p_i c_i \tag{4}$$

in which p_i=probability of occurrence of size fraction i of bed material; Σ=summation over N fractions; and N=number of size fractions.

The concentration profile is determined for each fraction using the fall velocity and β-factor of the fraction values. The turbulence damping, flocculation, and hindered settling parameters (see Van Rijn 2007b) are based on the fractional concentrations for reasons of simplicity, which is a reasonable assumption for the lower regime (effects are small anyway). In the upper regime, the total concentration summed over the fractions should be used requiring iterative computations. If time derivatives are involved, the total concentration of previous times ($t-\Delta t$) can be taken.

Sensitivity computations show that at least seven fractions (N=7) are required for accurate results in the low velocity range. Using N=3, 5, 7, and 12 fractions for d_{50}=200 μm (d_{10}=90 μm, d_{90}=310 μm, see Table 1) and h=3 m, u=0.5 m/s yields a suspended load transport of, respectively, q_s=0.00168, 0.00156, 0.0078, and 0.008 kg/s/m. The transport rate is about the same for $N \geqslant 7$.

Both the bed load transport and the suspended transport (through the reference concentration) strongly depend on the dimensionless bed-shear stress parameter T, defined as: $T=(\theta'-\theta_{cr})/\theta_{cr}=(\tau'_b-\tau_{b,cr})/\tau_{b,cr}$ for uniform sediment (see Van Rijn 2007b). In conditions with graded sediment it is not trivial in what way the T parameter should be modeled. Various methods were studied extensively by Van Rijn (2000) and Kleinhans and Van Rijn (2002). Herein, four methods are explored:

$$\text{Method A:} \quad T_i = \lambda_i[\tau'_b - \xi_i(d_i/d_{50})\tau_{b,cr,d_{50}}/(d_i/d_{50})\tau_{b,cr,d_{50}}] \tag{5a}$$

with τ'_b=effective bed-shear stress due to currents and waves $=\mu_c\tau_{b,c}+\mu_w\tau_{b,w}$ (see Van Rijn 2007b) and $\tau_{b,cr,d_{50}}$=critical shear stress based on d_{50}; $\xi_i=[\log(19)/\log(19d_i/d_{50})]^2$=hiding-exposure factor according to Egiazaroff (1965); $\lambda_I=(d_i/d_{50})^{0.25}$ =correction factor of effective grain-shear stress. This latter parameter represents the effect of modified grain-shear stress parameter in the case of graded beds, because the larger particles ($\lambda > 1$) are more exposed and experience larger fluid drag, whereas the smaller particles ($\lambda < 1$) are less exposed and experience smaller fluid drag. The effective grain-shear stress (τ'_b) involves a current-related efficiency factor (μ_c), which is related to the d_{90} of the mixture or the fraction size d_i and a wave-related efficiency factor (μ_w), which is related to the fraction size (d_i); (see Van Rijn 2007b).

For comparison the results of three other approaches (B, C, and D methods) will also be shown, being

$$\text{Method B:} \quad T_i = [\theta'_i - \xi_i\theta_{cr,d_{50}}]/\theta_{cr,d_{50}} = [\tau'_b - \xi_i(d_i/d_{50})\tau_{b,cr,d_{50}}]/[(d_i/d_{50})\tau_{b,cr,d_{50}}] \tag{5b}$$

with $\theta'_i=\tau'_b/[(\rho_s-\rho)gd_i]$=effective mobility parameter; $\theta_{cr,d_{50}}=\tau_{b,cr,d_{50}}/[(\rho_s-\rho)gd_{50}]$=critical mobility parameter based on d_{50}; τ'_b=effective bed-shear stress; $\tau_{b,cr,d_{50}}$=critical shear stress based on d_{50} (d_{50} method); and ξ_i=exposure factor according to Egiazaroff. Method B [used by Kleinhans and Van Rijn (2002)] is similar to Method A but the λ correction is not applied.

$$\text{Method C:} \quad T_i = [\theta'_i - \xi_i\theta_{cr,d_i}]/\theta_{cr,d_i} = [\tau'_b - \xi_i\tau_{b,cr,d_i}]/\tau_{b,cr,d_i} \tag{5c}$$

$$\text{Method D:} \quad T_i = [\theta'_i - \theta_{cr,d_i}]/\theta_{cr,d_i} = [\tau'_b - \tau_{b,cr,d_i}]/\tau_{b,cr,d_i} \tag{5d}$$

with $\theta'_i=\tau'_b/[(\rho_s-\rho)gd_i]$=effective mobility parameter; $\theta_{cr,d_i}=\tau_{b,cr,d_i}/((\rho_s-\rho)gd_i)$=critical mobility parameter based on d_i; τ_{b,cr,d_i}=critical shear stress based on d_i (d_i method); and ξ_i=exposure factor according to Egiazaroff. Method C is based on the fraction diameters (d_i method) without roughness correction. Method D is also based on the fraction diameters, but no correction is applied.

It is not quite clear how the grain roughness should be modeled in case of graded sediment mixtures. Two situations may occur: well-mixed bed material or nonmixed bed material with segregation of the individual fractions. In the case of well-mixed bed material the application of a constant grain roughness $k_{s,grain}=\alpha d_{90}$ [α=1–3; Van Rijn (1993); herein α=1] seems to be the most logical approach. In the case of bimodal bed material consisting of segregated fractions it may be better to relate the grain roughness to the size of the individual fractions of the bed material mixture ($k_{s,grain,i}=d_i$). The effect of the grain roughness on the transport rates according to the MF method has been studied by using $k_{s,grain,i}=d_i$ instead of $k_{s,grain}=d_{90}$. The latter approach implies a constant grain roughness and hence grain-shear stress (τ'_b) for all fractions. The grain roughness of $k_{s,grain}=d_{90}$ yields somewhat larger suspended load transport rates and hence larger total transport rates than that based on $k_{s,grain,i}=d_i$. Herein, both

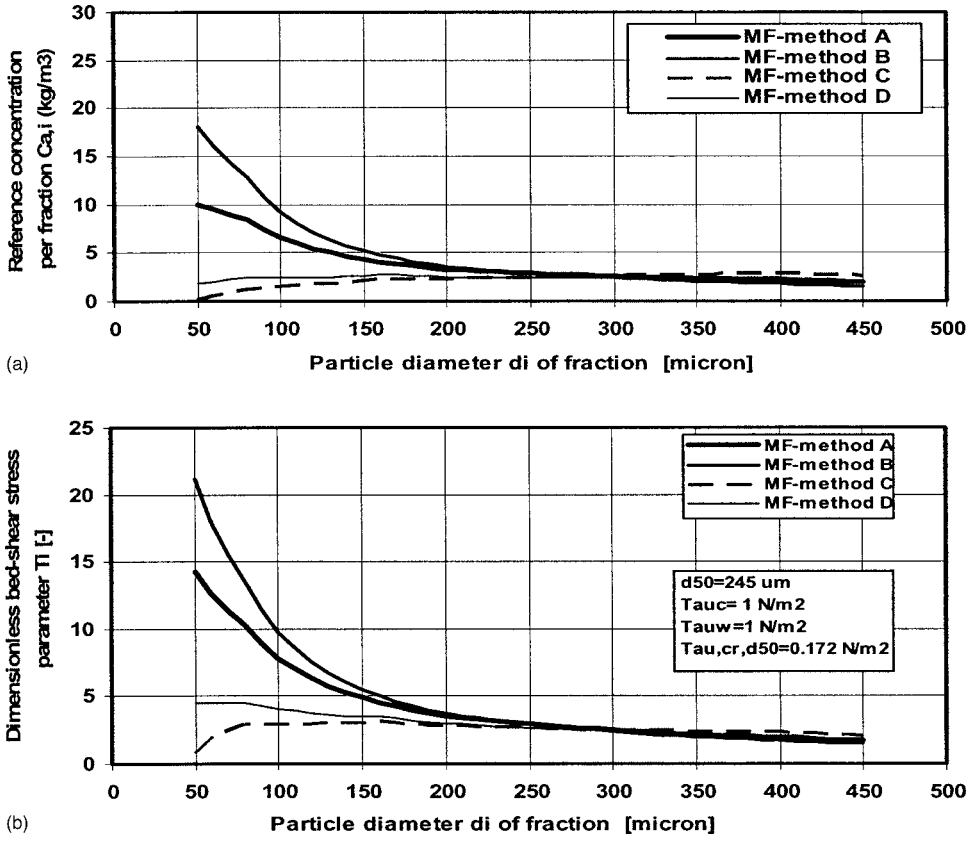

Fig. 4. Computed reference concentration (b); T-parameter per fraction (a) based on four different definitions of bed-shear stress parameter ($k_{s,\text{grain}}=d_{90}$)

grain roughness methods will be studied. This effect is especially important for very graded bed materials (sand-gravel beds), which is, however, not the focus of this paper.

Reference Concentration

The reference concentration for graded bed material reads as

$$c_a = 0.015 f_{\text{silt},i}(d_i/a)(D_{*,i})^{-0.3}(T_i)^{1.5}$$
$$\text{with } c_a \leq 0.05 \text{ (approx. 130 kg/m}^3\text{)} \qquad (6)$$

in which (see also Van Rijn 2007b) $D_{*,i}=d_i[(s-1)g/\nu^2]^{1/3}$ =dimensionless particle parameter of fraction i (-); s=relative density; ν=kinematic viscosity coefficient; T_i=dimensionless bed-shear stress parameter of fraction i (-); a=reference level (m), see Van Rijn 2007b; and $f_{\text{silt},i}=d_{\text{sand}}/d_i$=silt factor ($f_{\text{silt},i}=1$ for $d_i>d_{\text{sand}}$).

The T_i values and associated reference concentration values according to MF Methods A, B, C, and D with grain roughness equal to $k_{s,\text{grain}}=d_{90}$ are shown in Fig. 4 for a practical case of relatively fine graded bed material: $\tau_{b,c}=1$ N/m^2; $\tau_{b,w}=1$ N/m^2; $\mu_c=0.5$; $\mu_w=0.7/D_{*,i}$ (see Van Rijn 2007b); and $d_{50}=245$ μm (using 41 fractions between 50 and 450 μm; fraction percentage is $p_i=0.0243$ for all i); and $\tau_{b,\text{cr},d_{50}}=0.172$ N/m^2. Methods A and B yield relatively large T_i values for the smaller fraction diameters (smaller than the d_{50}) and relatively small T_i values for the larger fraction diameters (larger than d_{50}). Method D yields slightly increasing T_i values for decreasing fraction diameters. Method C yields slightly decreasing values for decreasing fraction diameters.

The fractional reference concentration [see Eq. (6)] is also shown in Fig. 4. The reference level is taken as $a=0.01$ m for this specific example. The reference concentration of the SF method SF is about 2.5 kg/m^3 for $d_{50}=245$ μm. The mean reference concentration values for the MF Methods A, B, C, and D are, respectively, 3.7, 4.6, 2.3, and 2.4 kg/m^3. It is a favorable feature of reference concentration function that all MF methods yield a mean reference concentration value within a factor of 2 of the SF method. Methods A and B yield values which are slightly larger than that of the SF method. The fractional reference concentrations of Method A vary weakly with the fractional diameter; between 10 kg/m^3 for $d_i=50$ μm and 2 kg/m^3 for $d_i=450$ μm. The fractional reference concentration is almost constant for the coarser particle size range >200 μm (Method A). Method C yields decreasing concentrations for the finer particle size range, which is not realistic. This is caused by the increase of the critical bed-shear stress for the finer particle size (see Fig. 4). The data of Tomkins et al. (2003) for suspension over natural rippled beds confirm that the concentrations are increasing for decreasing sediment diameter.

Suspended Transport Rate

The effect of the bed-shear stress parameter on the suspended transport has been studied by performing sensitivity computations using MF Methods A, B, C, and D. For reference the transport according to the SF method is also given. These computations have been made for four graded beds (40, 200, 400, and 800 μm, see Table 1) using as grain roughness $k_s=d_i$. The following flow

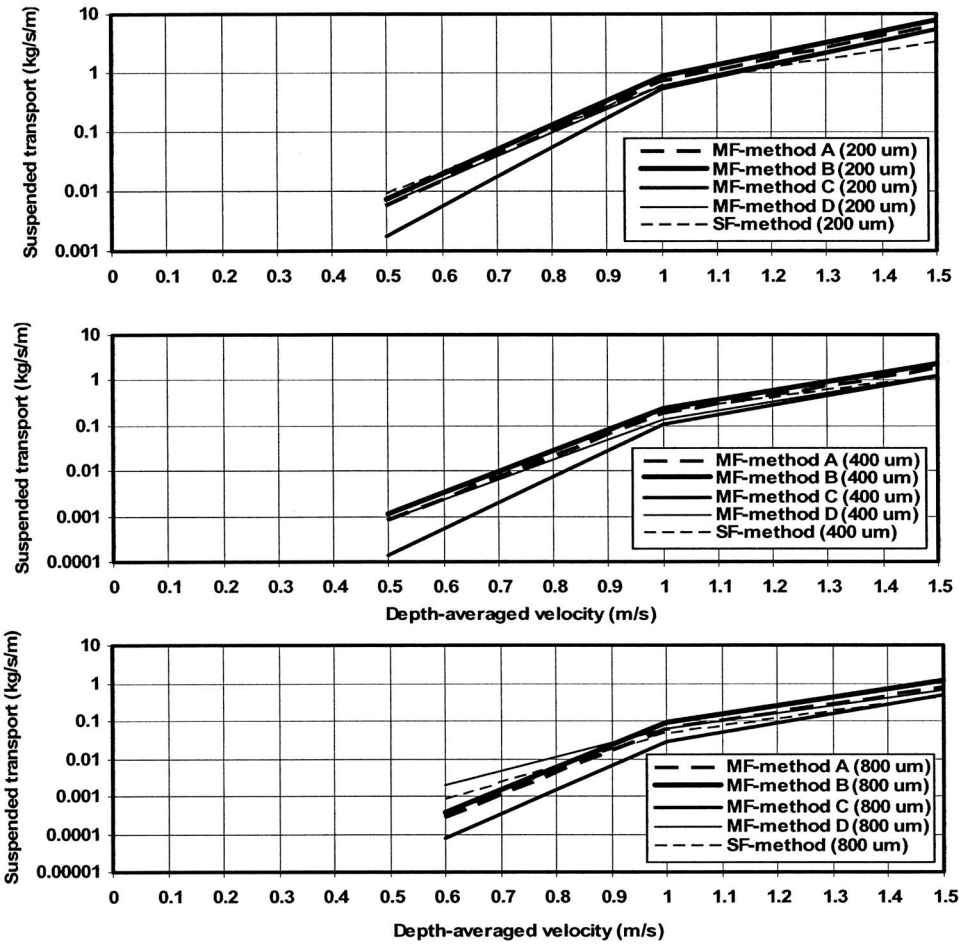

Fig. 5. Computed suspended load transport based on four different definitions of bed-shear stress parameter ($k_{s,\text{grain}}=d_i$), sediment of 200, 400, and 800 μm

conditions are considered: current velocity in the range of 0.5–1.5 m/s and water depth of 3 m. The water temperature is 15°C and the salinity is 30 promille.

The results for the 200, 400, and 800 μm beds are shown in Fig. 5 and for the 40 μm bed in Fig. 6. MF Method B yields the largest suspended load transport rates in most cases, whereas Method C yields the smallest values in line with the results presented in Fig. 4. The differences between the results of Methods A–D are smallest (within 50% for 40 μm sediment and within factor 2 for 200 to 800 μm) for relatively large velocities (>1 m/s), because the influence of the critical bed-shear stress (and hence influence of the hiding exposure factor) reduces for increasing velocities and hence bed-shear stresses. The differences are largest for 800 μm and a low velocitity of 0.6 m/s. In the latter case, Method D yields a suspended transport rate which is 20 times larger than that of Method C. The effect of the grain roughness method is relatively small for fine sediment beds (40 and 200 μm). Using $k_s=d_{90}$ for 40 and 200 μm results in suspended transport rates which are, on average, 30–50% larger than those based on $k_s=d_i$. For sediment beds of 400 and 800 μm the variations related to $k_s=d_{90}$ or $k_s=d_i$ increase to a factor of 2 (high-velocity range) to 3 (low-velocity range). The values of the SF method are very close (within 30%) to those of the MF methods for the 40 μm bed and velocities larger than 1 m/s. The SF method produces realistic suspended transport rates for sediment beds of 200 and 400 μm; (Van Rijn 2007b) the SF transport rates

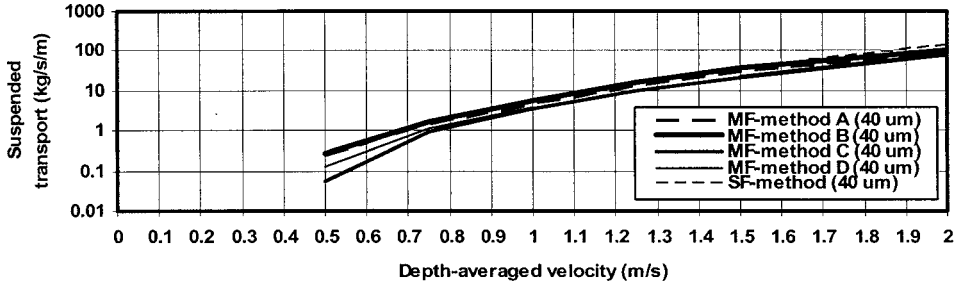

Fig. 6. Computed suspended load transport based on four different definitions of bed-shear stress parameter ($k_{s,\text{grain}}=d_i$), sediment of 40 μm

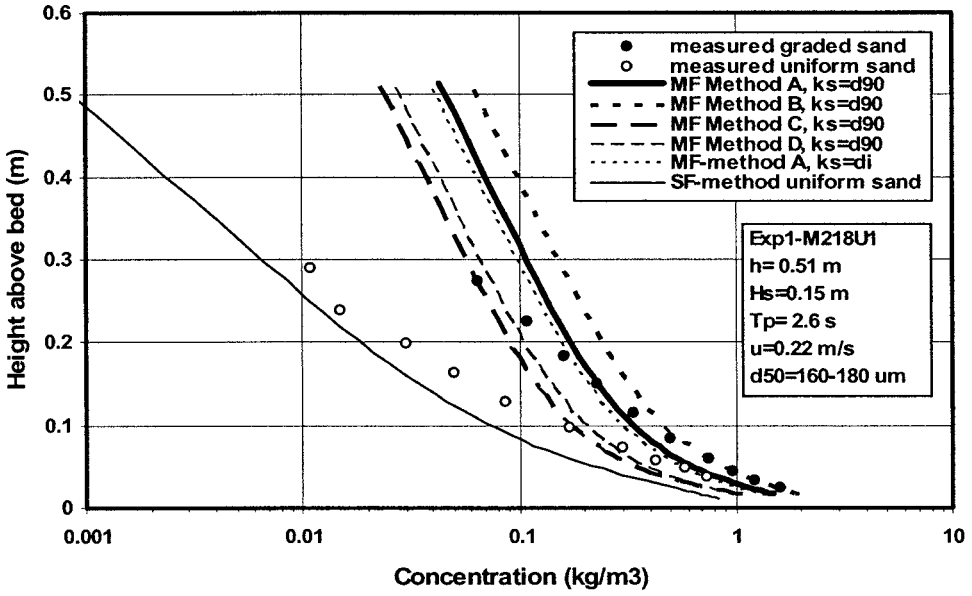

Fig. 7. Measured and computed concentration profiles for Tests M218U1 and 1-1G; uniform and graded beds

generally are somewhat too small (factor of 2) for larger velocities (>1 m/s) and somewhat too large (factor of 2) for smaller velocities (<0.75 m/s). Based on this, it can be concluded that the suspended size predictor (see Van Rijn 2007b) produces realistic results for sediment beds smaller than about 500 μm. MF methods are required for very graded coarse beds (>500 μm). Overall, Method C is not preferred herein, because Method C yields relatively small concentrations in the fine fraction range (see Fig. 4). Method B yields relatively large concentrations in the upper part of the water depth.

Comparison with Measured Data: Steady Flow with Waves

Experiments over a horizontal sand bed have been carried out in a small-scale wave-current flume of the Fluids Mechanics Laboratory of the Delft University of Technology (Jacobs and Dekker 2000; Sistermans 2000, 2002). Two types of sand have been used: uniform sand with d_{50} of about 0.16 mm and graded sand with d_{50} of about 0.25 mm. The water depth was about 0.5 m in all tests. The hydrodynamic conditions are irregular waves superimposed on a following current. The significant wave heights are in the range of 0.12–0.2 m. The depth-averaged current velocities are in the range of 0.1–0.3 m/s (following current). Time-averaged suspended sand concentrations and suspended transport rates have been measured. Instantaneous velocities and sand concentrations at various elevations above the bed have been measured by use of an acoustic instrument. Instantaneous fluid velocities have also been measured by use of an electromagnetic velocity meter. Time-averaged sand concentration profiles have been obtained by using a pump sampling instrument consisting of 10 intake tubes (internal opening of 3 mm; sampling time of about 20 min). The suspended sand sizes based on analysis in a settling tube are about d_s=0.7–0.9 $d_{50,\text{bed}}$ for the uniform bed materials (U-Tests) and about d_s=0.35–0.45 $d_{50,\text{bed}}$ for the graded bed material (G-Tests). The ripple height (r) is about 0.015–0.02 m and the ripple length is about 0.15–0.2 m in these tests. The temperature is 23–25°C. Herein, the following six tests have been used:

- Test 1-1G: h=0.515 m, H_s=0.147 m, T_p=2.5 s, u=0.22 m/s, d_{10}=85 μm, d_{50}=180 μm, d_{90}=395 μm; ten fractions (10% each): 75, 95, 130, 180, 230, 275, 305, 335, 375, and 450 μm;
- Test M218U1: h=0.506 m, H_s=0.152 m, T_p=2.6 s, u=0.22 m/s, d_{10}=115 μm, d_{50}=160 μm, d_{90}=240 μm;
- Test 2-1G: h=0.518 m, H_s=0.189 m, T_p=2.7 s, u=0.21 m/s, d_{10}=85 μm, d_{50}=210 μm, d_{90}=400 μm; ten fractions (10% each): 75, 92, 112, 145, 187, 240, 292, 330, 370, and 450 μm;
- Test M220U1: h=0.516 m, H_s=0.191 m, T_p=2.7 s, u=0.2 m/s, d_{10}=145 μm, d_{50}=195 μm, d_{90}=260 μm;
- Test M218G: h=0.5 m, H_s=0.155 m, T_p=2.7 s, u=0.2 m/s, d_{10}=90 μm, d_{50}=260 μm, d_{90}=420 μm; ten fractions (10% each): 75, 105, 130, 175, 230, 285, 325, 365, 400, and 450 μm; and
- Test M220G: h=0.5 m, H_s=0.155 m, T_p=2.7 s, u=0.2 m/s, d_{10}=90 μm, d_{50}=260 μm, d_{90}=420 μm; ten fractions (10% each): 75, 105, 130, 175, 230, 285, 325, 365, 400, and 450 μm.

Fig. 7 shows measured sand concentration profiles (based on the pumped concentrations) for uniform and graded bed material (same d_{50}) with H_s=0.15 m and u=0.22 m/s. As can be observed, the sand concentrations are largest for the graded sediment bed. The near-bed concentrations are about 50% larger for the graded sediment bed; the sand concentrations higher up in the water column are much larger (factor of 2–4) for the graded sediment bed, which is caused by the winnowing of the fine sediments from the bed.

MF Methods A–D (ten fractions) and the SF method have been used to compute the concentration profile for the graded sand bed. The results are shown in Fig. 7. Method B yields the largest reference concentration in good agreement with the measured near-bed concentration. Methods A, C, and D yield values which are somewhat too small. Method D yields almost the same results as Method C. The concentrations measured higher up in the water column are overpredicted by Method B. The effect of the grain roughness is rather small. Method A based on $k_{s,\text{grain}}=d_{90}$ and on $k_{s,\text{grain}}=d_i$ yields almost the same results.

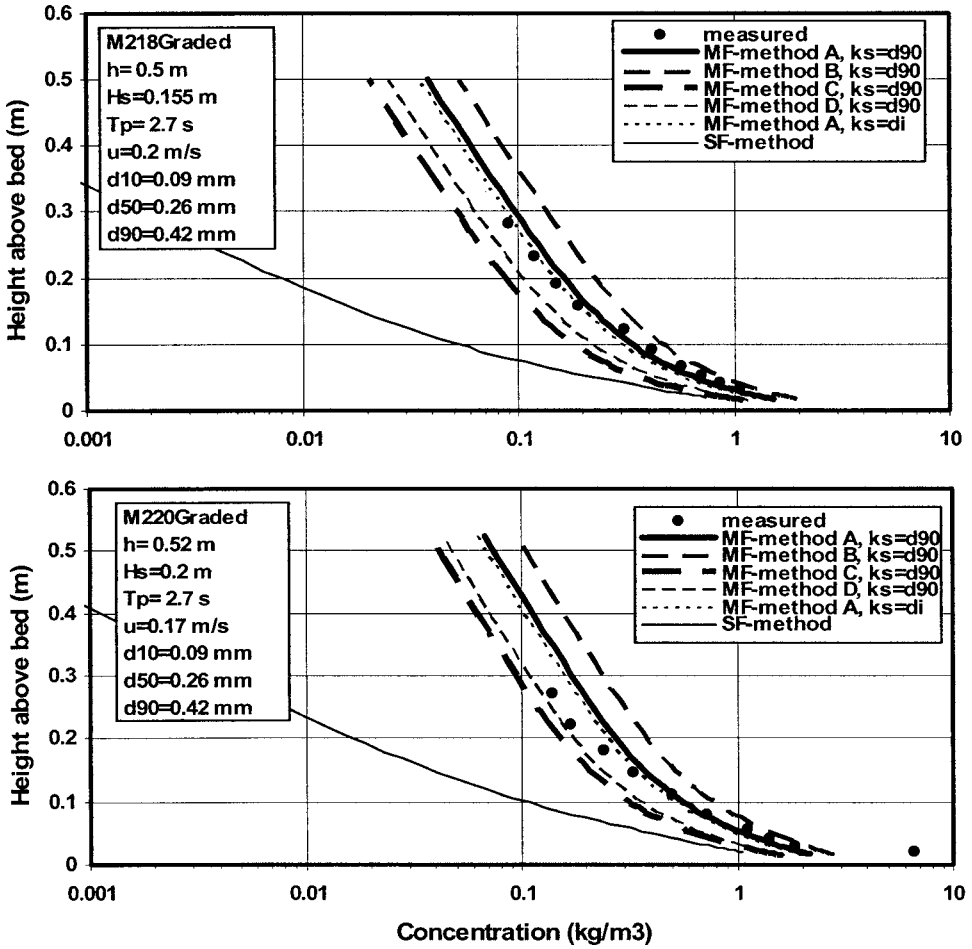

Fig. 8. Measured and computed sand concentration profiles for Tests M218G and M220G; graded beds

Fig. 8 shows measured sand concentration profiles (based on the pumped concentrations) for two tests (M218G and M220G) with graded bed material. Both the SF method and MF Methods A–D have been applied to compute the sand concentration profiles. The computed sand concentrations based on MF Method A show reasonably good agreement with the measured concentrations for the graded sand; the vertical distribution is rather well represented, but the reference concentration is somewhat underpredicted. Method B overpredicts the concentrations for both tests. Methods C and D underpredict the concentrations for both tests. The effect of the grain roughness (d_{90} or d_i) is marginal. The SF method severely underpredicts (factor of 5–10) the measured concentrations; the predicted suspended sediment size is about 175 μm whereas the measured value is about 110 μm. All MF methods yield larger concentrations than the SF method. Overall, MF Method A yields the best results. The SF method should not be used for very graded sediments ($d_{90}/d_{10}>4$).

Finally, it is remarked that only the case of a following current has been considered, because measured data of graded beds in other cases with opposing currents or arbitrary angles are not available. These latter cases are not supposed to show a significantly different effect, as Van Rijn (1993, Fig. 9.2.8) has shown that the magnitude of the suspended sand transport is not so much affected (within a factor of 2) by the angle between the wave and current direction, although the vertical structure of the flow in the upper half may be significantly different. The reason for this is that most of the sediment is transported in the lower half of the depth.

Comparison with Measured Data: Steady River Flow

MF Methods A and B based on $k_s=d_i$ have been used to compute the suspended transport rates for the field data (d_{50}=400–600 μm) shown in Fig. 4 of Van Rijn 2007b. The water depth is taken to be h=7 m. The bed material is schematized into six fractions (more fractions are required for the low-velocity range just beyond initiation of motion). The results of Methods A and B are presented in Fig. 9, showing similar results as the SF method (Van Rijn 2007b). Both methods yield good results using $k_s=d_i$, whereas the use of $k_s=d_{90}$ yields somewhat larger transport rates (about 50%).

The field data set of Anderson (1942) has also been used to test the MF methods. He collected suspended sediment samples in the Enoree River in the United States. At the point of collection the river was straight and regular with almost vertical banks (width of 15 m). The sand bed consisted of graded bed material with sizes in the range of 60–5,000 μm. The sediment characteristics were found to be: d_{10}=320 μm; d_{50}=655 μm; d_{90} =1,300 μm. Based on the available data (percentages of very fine fractions were very small), the bed material has been represented by eight fractions as follows: 100 μm (0.5%), 150 μm (1%), 210 μm (1.5%), 300 μm (4.5%), 420 μm (15%), 600 μm (22.5%), 850 μm (22.5%), and 1,500 μm (32.5%). The water depth was in the range of 0.9–1.5 m; the flow velocity was in the range of 0.55–0.85 m/s. The water surface slope was determined from two recording gauges located about 300 m apart at the upper and lower ends of the reach (S=0.00074). The effective bed-

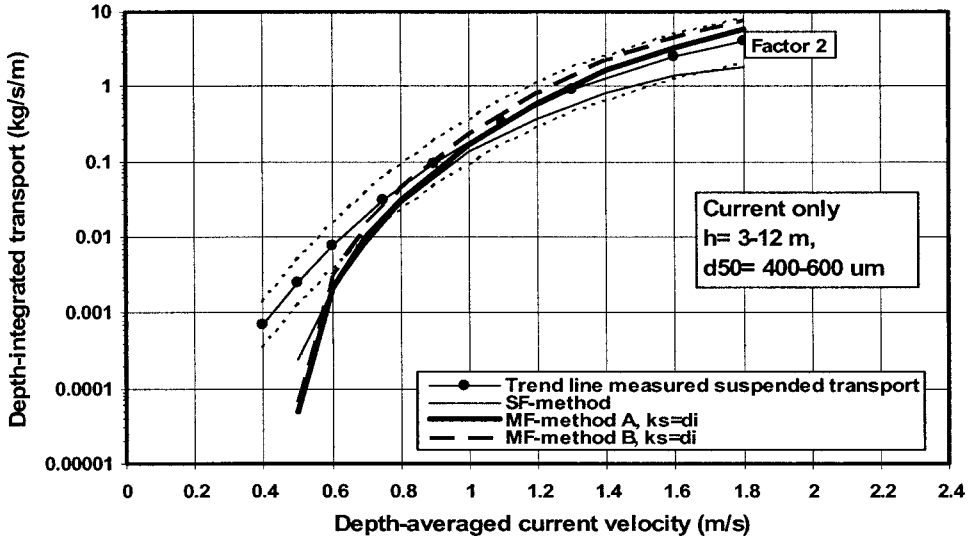

Fig. 9. Measured and computed suspended transport for sediments in the range of 400–600 μm (d_{10}=100 μm, d_{50}=500 μm, d_{90}=900 μm)

roughness values are rather large suggesting the presence of large-scale bed forms (dunes). The suspended sediment sampler consisted of a number of pint milk bottles attached at regular intervals to a cable.

Data of the following two cases have been used:

1. February 19, 1940 SN 2.40: h=1.52 m/s, u=0.85 m/s, k_s=0.7 m, Te=8 °C; and
2. February 19, 1940 SN 17.00: h=1.28 m/s, u=0.75 m/s, k_s=0.8 m, Te=8 °C.

Sand concentration profiles have been computed for these two cases using four MF Methods (A–D) and N=8 fractions. The SF method (Van Rijn 2007b) has also been used. The measured and computed concentrations are shown in Fig. 10. The near-bed concentrations are substantially overpredicted (factor of 2), but the

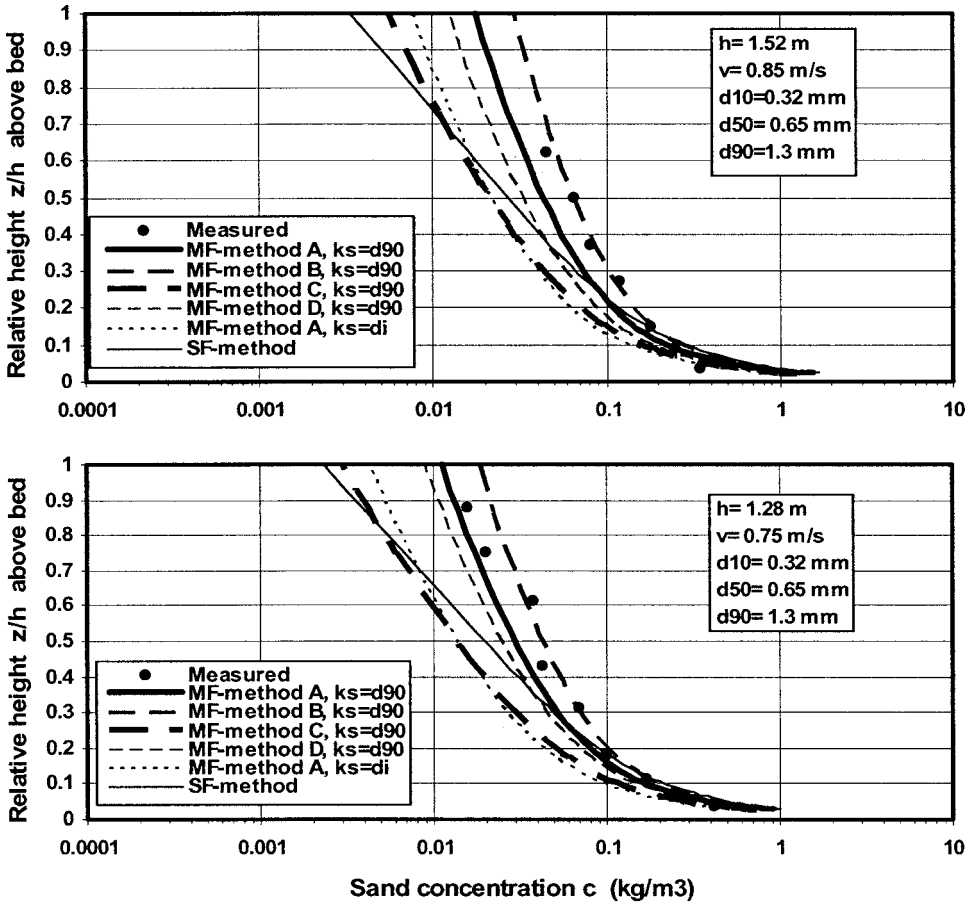

Fig. 10. Measured and computed sand concentration profiles for steady river flow: Enoree River

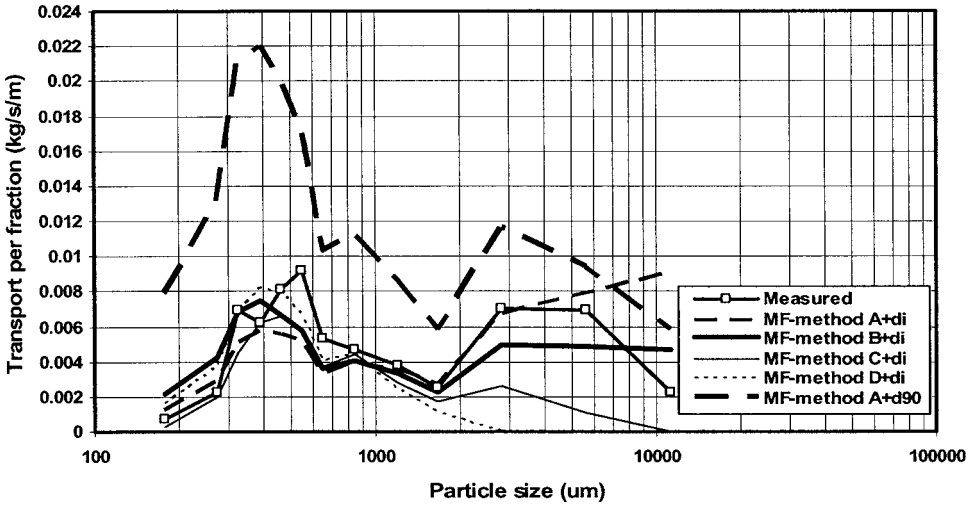

Fig. 11. Comparison of measured and computed transport per fraction in flume, Test T7

sand concentrations in the upper portion of the flow depth are rather well represented by MF Methods A and B using $k_{s,\text{grain}}=d_{90}$. MF Method D also yields reasonable results. Method A based on $k_{s,\text{grain}}=d_i$ yields concentrations which are systematically too small (factor of 2 to 3). The SF method gives overpredicted concentrations in the lower part of the depth and underpredicted concentrations in the upper part (within a factor of 2). It is noted that the computed near-bed concentrations represent a spatially averaged value along the bed forms, whereas the measured concentrations are local values at some location along the bed forms.

Bed-Load Transport

The bed load transport equation for graded bed material reads as (see Van Rijn 2007a)

$$q_b = 0.5\rho_s f_{\text{silt},i} d_i [D_{*,i}]^{-0.3} [\tau'_{b,\text{cw}}/\rho]^{0.5} [T_i] \quad (7)$$

in which $\tau'_{b,cw}$=instantaneous grain-related bed-shear stress due to both currents and waves=$0.5\ \rho_w f'_{cw}(U_{\delta,cw})^2$; $U_{\delta,cw}$=instantaneous velocity due to currents and waves at edge of wave boundary layer; f'_{cw}=grain friction coefficient due to currents and waves $=\alpha\beta f'_c+(1-\alpha)f'_w$; f'_c=current-related grain friction coefficient based on $k_{s,\text{grain}}=d_{90}$ or d_i; f'_w=wave-related grain friction coefficient based on $k_{s,\text{grain}}=d_{90}$ or d_i; α=coefficient related to relative strength of wave and current motion (Van Rijn 1993); β=coefficient related to vertical structure of velocity profile (Van Rijn 1993); T_i=bed-shear stress parameter [see Eq. (5)]; sediment ρ_s=density; ρ_w=fluid density; d_i=particle size of fraction i; $D_{*,i}$=dimensionless particle size of fraction i; and $f_{\text{silt},i}=d_{\text{sand}}/d_i$ =silt factor ($f_{\text{silt}}=1$ for $d_i>d_{\text{sand}}$).

Effect of Bed-Shear Stress Parameter

The effect of the bed-shear stress parameter on the bed load transport has been studied by performing sensitivity computations using MF Methods A, B, C, and D and also the SF method. These computations have been made for three graded beds: 200, 400, and 800 μm (see Table 1). Three flow conditions are considered: current velocity=0.5, 1.0, and 1.5 m/s and a water depth=3 m. The water temperature is 15°C and the salinity is 30 promille. The results show that the bed load transport rates are within 20% for most cases (not shown). Method A yields the largest values, whereas Method C yields the smallest values. The effect of the bed-shear stress parameter on the bed load transport is not so large, because of the weak effect of particle diameter on bed load transport (see Van Rijn 2007a). The differences are larger for velocities (0.5 m/s) just beyond the critical bed-shear stress in the case with a sediment bed of 800 μm. Method C yields relatively small values (factor 3 smaller). The SF method yields realistic values compared with MF Methods A, B, and D for all cases (within 10%) for sediment beds of 200 and 400 μm and within a factor of 2 for a sediment bed of 800 μm. Hence, the application of a MF method is less important for beds smaller than about 500 μm, because of relatively good sorting and near-equal mobility of the sediment fractions.

Comparison with Measured Data: Steady Flow in Flume

Kleinhans and Van Rijn (2002) have studied the transport of sand-gravel mixtures (0.15–11.3 mm) in a large-scale flume, both for incipient motion and for fully mobile conditions. The test results for incipient motion cannot be modeled by the present method, as these results basically require a stochastic model approach. However, the results of Test T7 concerns fully mobile bed conditions and have been used to verify the present deterministic MF Methods A–D using $k_{s,\text{grain}}=d_{90}$ and $k_s=d_i$. The basic data of Test T7 are: depth=0.31 m; velocity=0.79 m/s; slope=17.7×10^{-4}; d_{10}=320; d_{50}=870; d_{90}=7,200 μm; q_t=0.066 kg/s/m.

The present transport model (13 fractions) yields:

- MF Method A with $k_{s,\text{grain}}=d_i$: q_t=0.063 kg/s/m;
- MF Method B with $k_{s,\text{grain}}=d_i$: q_t=0.061 kg/s/m;
- MF Method C with $k_{s,\text{grain}}=d_i$: q_t=0.042 kg/s/m;
- MF Method D with $k_{s,\text{grain}}=d_i$: q_t=0.047 kg/s/m; and
- MF Method A with $k_{s,\text{grain}}=d_{90}$: q_t=0.154 kg/s/m.

All methods based on $k_s=d_i$ yield values of the right order of magnitude. Methods A and B with $k_{s,\text{grain}}=d_{90}$ significantly overpredicts (factor of 2 to 3) the total transport rates, basically because the bed-shear stress acting on the fine fractions is too large. Fig. 11 presents the transport rates per fraction. Methods A and B with $k_s=d_i$ produce total transport rates, which are very close to the measured value of 0.066 kg/s/m. Method A with $k_s=d_i$ underpredicts the transport rate of the smaller fraction sizes and

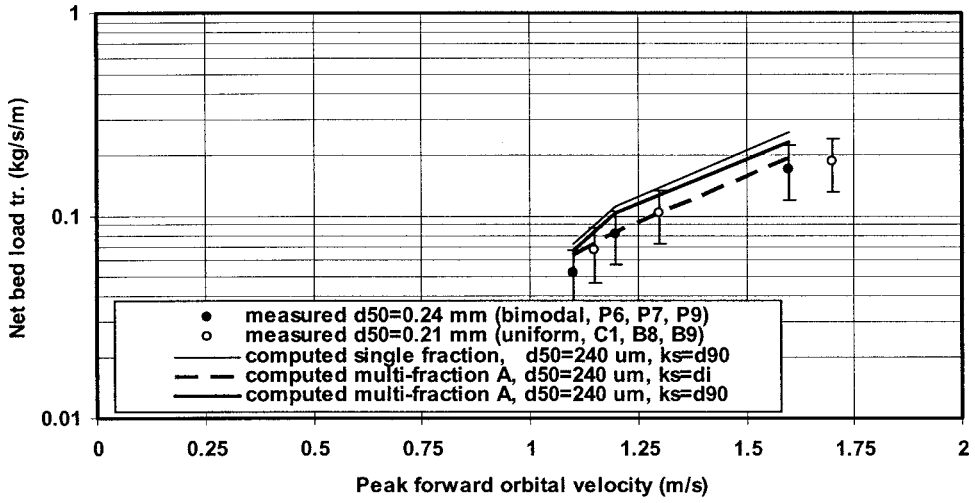

Fig. 12. Comparison of measured and computed bed-load transport rates in wave tunnel; effect of graded bed material

overpredicts for the larger fraction sizes. Method B with $k_s=d_i$ yields very reasonable results over the full size range. Methods C and D with $k_s=d_i$ significantly underpredict the transport rates of the larger fraction sizes.

Comparison with Measured Data: Steady Flow in East Fork River, United States

Leopold and Emmett (1976, 1977) have studied the transport of sand-gravel mixtures (0.2–50 mm) in the East Fork River in Wyoming. The transport was measured by using a conveyer belt bed load trap across the river. Herein, the group average values of one high flow condition are used [see Kleinhans and Van Rijn (2002)]. The basic data are: depth=1.32 m; velocity=1.29 m/s; d_{10}=350; d_{50}=1,050; d_{90}=3,600 μm; and q_t=0.136 kg/s/m (60% sand and 40% gravel). Using the particle size distribution of the transported bed material, the present transport model yields

- MF Method A with $k_{s,\text{grain}}=d_i$: q_t=0.249 kg/s/m (78% sand <2 mm and 22% gravel >2 mm) and
- MF Method B with $k_{s,\text{grain}}=d_i$: q_t=0.276 kg/s/m (85% sand <2 mm and 15% gravel >2 mm).

Both methods based on $k_s=d_i$ overpredict the measured transport rate by a factor of 2. In particular, the amount of sand transport is overpredicted. Method A yields somewhat better results than Method B. Using $k_s=d_{90}$ will result in even larger overprediction.

Comparison with Measured Data: Oscillatory Flow in Wave Tunnel

Three tests (P6, P7, P9) have been carried out in the wave tunnel of Delft Hydraulics (Hassan et al. 1999) for a bimodal sand consisting of 210 μm (70%) and 970 μm (30%). The d_{50} is about 240 μm and the d_{90} is about 900 μm. All experimental results are in the sheet flow regime. The measured net bed load transport rates under conditions of asymmetric wave motion are as follows (see Fig. 12):

- P6: U_{for}=1.09 m/s, U_{back}=0.57 m/s, T=6.5 s, $q_{b,\text{fine}}$=0.029 kg/s/m, $q_{b,\text{coarse}}$=0.023 kg/s/m, q_t=0.051 kg/s/m;
- P7: U_{for}=1.23 m/s, U_{back}=0.65 m/s, T=6.5 s, $q_{b,\text{fine}}$=0.041 kg/s/m, $q_{b,\text{coarse}}$=0.040 kg/s/m, q_t=0.081 kg/s/m; and
- P9: U_{for}=1.60 m/s, U_{back}=0.85 m/s, T=6.5 s, $q_{b,\text{fine}}$=0.08 kg/s/m, $q_{b,\text{coarse}}$=0.09 kg/s/m, q_t=0.17 kg/s/m.

U_{for} and U_{back} are the peak orbital velocities in forward and backward direction of the sinusoidal wave propagation. The results of Tests P6, P7, and P9 are shown in Fig. 12. For comparison the results of Tests C1, B8, and B9 with uniform sand of 0.21 mm are also shown in Fig. 12. As can be observed, the measured net transport rates of uniform and graded sediment are almost the same (within error range). Thus, the presence of a coarse fraction (30% with diameter of 970 μm) has almost no influence on the net transport rate. The bed load transport model has been used to compute the net transport rates using the SF and the MF approaches. To apply the MF method, the bed mixture has been schematized in three fractions: two fine fractions (30% of d_1=180 μm and 40% of d_2=300 μm) and one coarse fraction (30% of d_3=970 μm). Four MF methods have been used (A–D) and two types of roughness methods ($k_s=d_{90}$ or $k_s=d_i$) have been used for Methods A and B. Using $k_s=d_{90}$, the grain-related bed-shear stress is the same for all fractions assuming well-mixed bed conditions. Using $k_s=d_i$, the grain-related bed-shear stress is related to the individual fraction diameter assuming segregation of the fractions. Segregation processes were observed during most tests. Initially the bimodal bed material in the tunnel was well mixed, but after the tests the coarser fraction was larger at the downwave end (in the direction of the largest peak orbital velocity; onshore direction) of the tunnel and smaller at the upwave end of the tunnel.

Methods A–D based on $k_s=d_{90}$ yield values which are within 20% of each other. All methods overestimate the measured transport by about 20–45%. The results of Method A with $k_s=d_{90}$ and $k_s=d_i$ are shown in Fig. 12. The bed load transport rates per fraction of Test P9 are shown in Fig. 13. The computed bed load transport of the fine fraction is obtained as $q_{b,\text{fraction1}}+q_{b,\text{fraction2}}$; the bed load transport of the coarse fraction is represented by the transport of fraction 3 ($q_{b,\text{fraction3}}$). Method A with $k_s=d_i$ yields the best results, because the bed load transport of the fine fraction is reasonably well represented, as shown in Fig. 13. Similar results are obtained for Tests P6 and P7 (not shown). The results of Method B are also shown in Fig. 13. The total bed load transport is quite well represented, but the bed load transport of the fine fractions is significantly overestimated and the transport of the

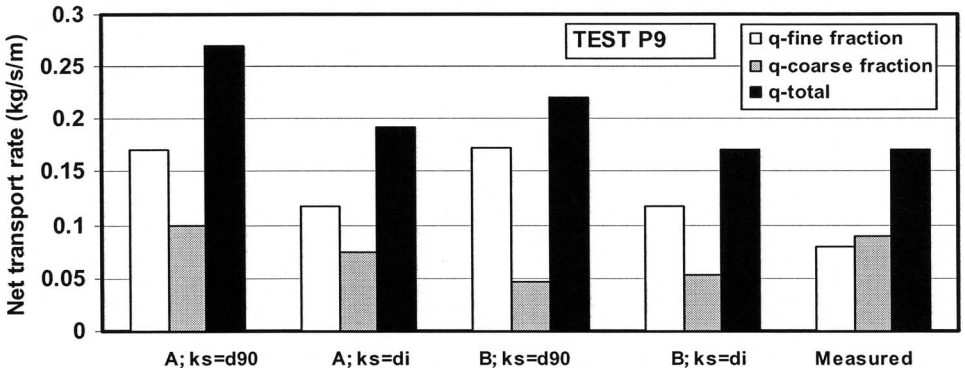

Fig. 13. Comparison of measured and computed bed-load transport per fraction; Wave Tunnel Test P9

coarse fraction is underestimated. Method D also yields reasonably good values, but the fine fraction is somewhat overestimated and the coarse fraction is underestimated (not shown). The single-fraction approach based on $d_{50}=240$ μm and $d_{90}=970$ μm yields an overestimation of about 40%, as can be seen in Fig. 12.

It is concluded for this wave tunnel case that the modeling of the grain roughness has the largest effect on the computed bed load transport. Using $k_s=d_i$ yields somewhat better results than $k_s=d_{90}$. The hiding factor is not important for the sheet flow regime (due to the presence of relatively large bed-shear stresses). The total transport rate can also be estimated with the SF method (slight overprediction).

Conclusions

The findings of the present study can be summarized in the following conclusions:

- The critical bed-shear stress for initiation of motion strongly depends on the degree of exposure of a grain with respect to surrounding grains. For steady flow in gravel-bed rivers it has been found that all sizes in a mixture begin to move at nearly the same bed-shear stress (equal mobility concept). For steady flow in graded sand-bed rivers the critical bed-shear stress of the finer fractions may be somewhat larger than those of the coarser fractions. The critical bed-shear stress of the fractions of graded bed material can be best represented by the critical Shields value based on the median particle diameter d_{50} and a hiding-exposure factor;
- Analysis of experimental results of uniform and graded beds with the same median particle size in a flume shows that the suspended load transport above a graded sand bed increases by a factor of 2 to 3 compared with that above an almost uniform sand bed;
- The sand transport for graded bed material can be computed by using a multifraction method (MF method); the sand transport rate of each size fraction of the bed material is computed using an existing single-fraction method (replacing the median diameter of the bed material by the mean diameter of each fraction) with correction factors to account for the nonuniformity effects. MF method (A) based on the hiding correction factor of Egiazaroff and a grain-shear stress correction factor seems to work reasonably well for steady flow with and without waves and is, therefore, used as the standard method of the TR2004 Model. The hiding factor is most important in the low shear stress regime just beyond initiation of motion. Method D yields very reasonable results for relatively fine sand (0–500 μm);
- The MF method yields about the same bed load transport rates as the SF method for sediments in the range of 100–500 μm. The MF method yields substantially larger suspended transport rates (factor of 2–10) than the SF method in case of a fine graded sand bed due to the relatively large contribution of the finer fractions to the total suspended transport rate. This latter finding is in line with the experimental results;
- In the case of well-mixed bed material the application of a constant grain roughness related to the d_{90} of the mixture seems to be the most logical approach ($k_s=d_{90}$). In the case of bimodal bed material (sand-gravel bed rivers) consisting of segregated fractions it is better to relate the grain roughness to the grain size of the individual fractions of the bed material mixture ($k_s=d_i$). Both methods yield similar results for the fine sand range. The latter method ($k_s=d_i$) yields the best results for very graded, coarse beds and is, therefore, used as the standard method of the TR2004 Model;
- The computed sand concentrations and transport rates based on the MF method are in reasonably good agreement with the measured values for experiments with graded sand in conditions with steady flow with and without waves; and
- The MF method should be used for $d_{90}/d_{10}>4$; about six to eight fractions should be used (more fractions for low velocity cases close to initiation of motion when part of the sediment may be immobile); the partitioning scheme (fraction sizes) should be based on the available sieve curve and on sensitivity computations (to obtain the proper converged transport rate).

In this series of three papers it has been shown that the deterministic TR2004 Model is a general transport model for uniform as well as graded beds and for steady flow in rivers as well as for combined steady and oscillatory flow of coastal waters. The model can be applied over the full silt and sand bed range from 8 to 2,000 μm. In the very coarse gravel range (>2,000 μm) it is essential to use a stochastic model approach instead of a deterministic approach [as proposed by Kleinhans and Van Rijn (2002)]. The present formulations for the bed load transport and the reference concentration can easily be reformulated in terms of stochastic parameters (Van Rijn 1987, 1993, 2005, 2007c). The transport data sets used show that TR2004 Model works rather well for these very diverse conditions. In another paper the performance of the TR2004 Model in a three-dimensional morphological model (DELFT3D Model) will be explored.

Acknowledgments

The National Institute for Coasts and Sea (RIKZ /Rijkswaterstaat, The Netherlands) is gratefully acknowledged for providing research funds within the Generic Coastal Research Programme (VOP). Also acknowledged are the Basic Research Programme of Delft Hydraulics and the European Research Projects SEDMOC, COAST3D, and SANDPIT sponsored by the European Community Research Programme. J. R. van den Berg and M. Kleinhans of the University of Utrecht are gratefully acknowledged for their critical comments on the manuscript.

References

Andersen, A. G. (1942). "Distribution of suspended sediment in a natural stream." *Transactions*, American Geophysical Union, Papers Hydrology, 678–682.

Buffington, J. M., and Montgomery, D. R. (1997). "A systematic analysis of eight decades of incipient motion studies with reference to gravel-bedded rivers." *Water Resour. Res.*, 33(8), 1993–2029.

Carling, P. A. (1983). "Threshold of coarse sediment transport in broad and narrow natural streams." *Earth Surf. Processes Landforms*, 8, 1–18.

Day, T. J. (1980). "A study of the transport of graded sediments." *Rep. No. IT 190*, HR Wallingford, U.K.

Egiazaroff, I. V. (1965). "Calculation of nonuniform sediment concentrations." *J. Hydr. Div.*, 91(4), 225–247.

Fenton, J. D., and Abbott, J. E. (1977). "Initial movement of grains on a stream bed: The effect of relative protrusion." *Proc. R. Soc. London, Ser. A*, 352, 523–537.

Hassan, W., Kroekenstoel, D. F., Ribberink, J. S., and Van Rijn, L. C. (1999). "Gradation effects on sand transport under oscillatory sheet flow conditions." *Rep. No. Z2099.10*, Delft Hydraulics, Delft, The Netherlands.

Jacobs, C., and Dekker, S. (2000). "Sediment concentrations due to currents and irregular waves: The effect of grading of the bed material." *Measurements Rep.*, Delft Univ. of Technology, Delft, The Netherlands.

Kleinhans, M. G., and Van Rijn, L. C. (2002). "Stochastic prediction of sediment transport in sand-gravel bed rivers." *J. Hydraul. Eng.*, 128(4), 412–425.

Komar, P. D. (1996). "Entrainment of sediments from deposits of mixed grain sizes and densities." *Advances in fluvial dynamics and stratigraphy*, P. A. Carling and M. R. Dawson, eds., Wiley, New York.

Kuhnle, R. A. (1993). "Incipient motion of sand-gravel sediment mixtures." *J. Hydraul. Eng.*, 119(2), 1400–1415.

Leopold, L. B., and Emmett, W. W. (1976). "Bed load measurements East Fork River, Wyoming." *Proc. Natl. Acad. Sci. U.S.A.*, 73(4), 1000–1004.

Leopold, L. B., and Emmett, W. W. (1977). "Bed load measurements East Fork River, Wyoming." *Proc. Natl. Acad. Sci. U.S.A.*, 74(7), 2644–2648.

Misri, R. L., Garde, L. J., and Ranga Raju, K. G. (1984). "Bed load transport of coarse nonuniform sediment." *J. Hydraul. Eng.*, 110(3), 312–328.

Parker, G., Klingeman, G. C., and McLean, D. G. (1982). "Bed load and size distribution in paved gravel-bed streams." *J. Hydr. Div.*, 108(4), 544–571.

Petit, F. (1994). "Dimensionless critical shear stress evaluation from flume experiments using different gravel beds." *Earth Surf. Processes Landforms*, 19, 565–576.

Rakoczi, L. (1975). "Influence of grain-size composition on the incipient motion and self-pavement of bed materials." *16th IAHR*, San Paulo, Brazil, 150–157.

Sistermans, P. J. G. (2000). "Net sediment transport measurements per fraction for well-graded sediment by irregular waves and a current: Data report." *Rep.*, Delft Univ. of Technology, Delft, The Netherlands.

Sistermans, P. J. G. (2002). "Graded sediment transport by non-breaking waves and a current." Doctoral thesis, Dept. of Civil Engineering, Delft Univ. of Technology, Delft, The Netherlands.

Tomkins, M. R., Nielsen, P., and Hughes, M. G. (2003). "Selective entrainment of sediment graded by size and density under waves." *J. Sediment Res.*, 73(6), 906–911.

Van Rijn, L. C. (1987). "Mathematical modelling of morphological processes in the case of suspended sediment transport." Doctoral thesis, Dept. of Fluids Mechanics, Delft Univ. of Technology, Delft, The Netherlands.

Van Rijn, L. C. (1993). *Principles of sediment transport in rivers, estuaries, and coastal seas*, Aqua, Blokzil, The Netherlands, ⟨www.aquapublications.nl⟩.

Van Rijn, L. C. (2000). "General view on sediment transport by currents and waves." *Rep. No. Z2899*, Delft Hydraulics, Delft, The Netherlands.

Van Rijn, L. C. (2005). *Principles of sedimentation and erosion engineering in rivers, estuaries, and coastal seas*, Aqua, Blokzil, The Netherlands, ⟨www.aquapublications.nl⟩.

Van Rijn, L. C. (2007a). "Unified view of sediment transport by currents and waves. I: Initiation of motion, bed roughness and bed-load transport." *J. Hydraul. Eng.*, 133(6), 649–667.

Van Rijn, L. C. (2007b). "Unified view of sediment transport by currents and waves. II: Suspended transport." *J. Hydraul. Eng.*, ASCE, 133(6), 668–689.

Van Rijn, L. C. (2007c). *Principles of sediment transport in rivers, estuaries and coastal seas* (update/supp;ement), Aqau, Blokzil, The Netherlands, ⟨www.aquapublications.nl⟩.

Wilcock, P. R. (1993). "Critical shear stress of natural sediments." *J. Hydraul. Eng.*, 119(4), 491–505.

Wilcock, P. R., and McArdell, B. W. (1993). "Surface-based fractional transport rates: Mobilization thresholds and partial transport of a sand-gravel sediment." *Water Resour. Res.*, 29(4), 1297–1312.

Wilcock, P. R., and Southard, J. B. (1988). "Experimental study of incipient motion in mixed-size sediment." *Water Resour. Res.*, 24(7), 1137–1151.